IJIRSET
International Journal of Innovative Research in Science | Engineering | Technology

ISSN(O): 2319-8753
ISSN(P): 2347-6710



International Journal of Innovative Research in Science Engineering and Technology (IJIRSET)

(A Monthly, Peer Reviewed, Refereed, Scholarly Indexed, Open Access Journal)



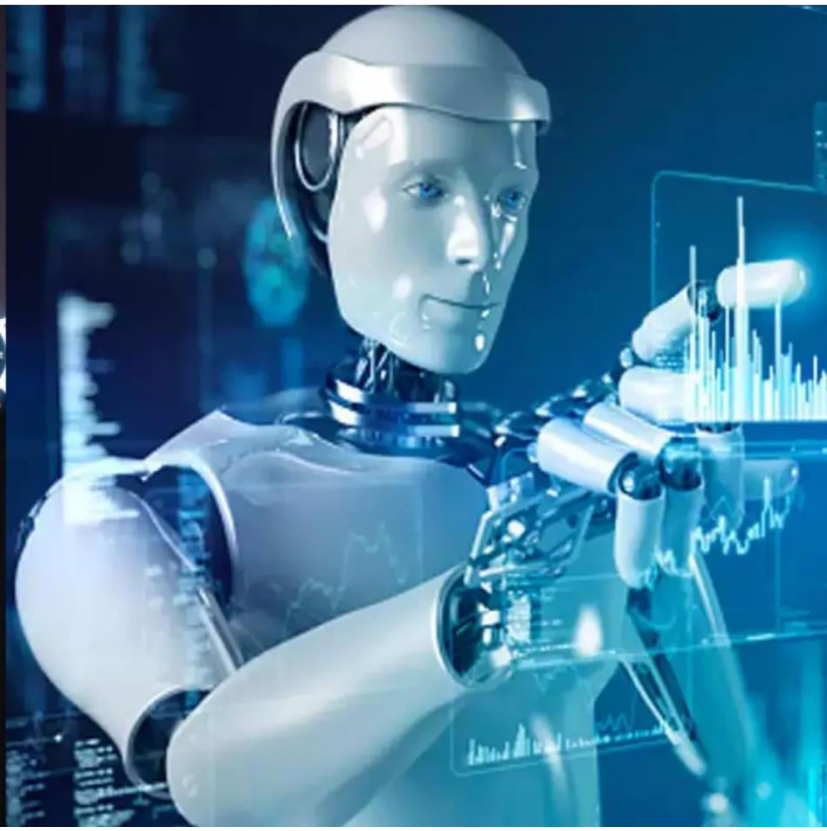

Impact Factor: 9.935

Volume 15, Issue 11, November 2026

International Journal of Innovative Research of Science, Engineering and Technology (IJIRSET)

Impact Factor 9.935

|www.ijirset.com |A Monthly, Peer Reviewed & Refereed Journal| e-ISSN: 2319-8753| p-ISSN: 2347-6710|

Volume 15, Issue 11, November 2026

|DOI: 10.15680/IJIRSET.2026.1511036|

Optimization of Submerged Arc Welding (SAW) Process Parameters using Taguchi Design of Experiments with Recycled Steel Slag Flux: Effect on Weld Bead Geometry and Flux Performance

Manish Sharma, Pankaj Arora

M. Tech Scholar, Department of Mechanical Engineering, Yamuna Institute of Engineering and Technology, Gadholi, Yamuna Nagar, Haryana, India

Assistant Professor, Department of Mechanical Engineering, Yamuna Institute of Engineering and Technology, Gadholi, Yamuna Nagar, Haryana, India

ABSTRACT: This paper applies the Taguchi design of experiments to optimize submerged arc welding (SAW) carried out with a recycled steel slag flux, prepared from slag recovered from earlier SAW deposits. Four process parameters — welding current, arc voltage, travel speed and nozzle-to-plate distance — were each varied at three levels in an L9 orthogonal array, reducing the 81 trials of a full factorial to nine. Penetration depth, bead width and reinforcement height were measured and converted to signal-to-noise (S/N) ratios (larger-the-better for penetration; smaller-the-better for bead width and reinforcement). Response tables, pooled-error ANOVA on the S/N data and a composite multi-response S/N index weighted toward penetration were used to rank the parameters and select the optimum. Welding current dominated penetration depth (74.0% contribution to S/N variation), while travel speed dominated reinforcement height (67.1%) and bead width (64.3%). The composite index gave an optimum of I = 500 A, V = 32 V, S = 24 m/hr and N = 31 mm (A3B3C3D3), for which the additive Taguchi model predicts a penetration of about 8.0 mm, a bead width of about 17.0 mm and a reinforcement height of about 4.7 mm; a confirmation run is required to verify these values. At the optimized parameters, the recycled steel slag flux produced welds that met AWS D1.1 / A5.17 acceptance criteria with tensile strength within about 3% of a commercial fused flux, at a raw-material cost reduction of approximately 30–54%.

KEYWORDS: Taguchi method, submerged arc welding, recycled steel slag flux, orthogonal array, S/N ratio, ANOVA, weld bead geometry

I. INTRODUCTION

Welding continues to be one of the most widely used metal-joining techniques in modern fabrication industries, valued for its efficiency, speed and economic advantages over alternative methods such as riveting and casting. Manufacturers are under constant pressure to produce reliable, high-quality components at the lowest possible cost, and the choice of joining process plays a central role in meeting this objective [1], [2].

An electric arc is struck between a constantly fed, bare or copper-coated consumable electrode and the workpiece in submerged arc welding (SAW), a fusion welding technique that produces metal coalescence. A layer of granular, fusible flux completely envelops the arc and the molten weld pool, protecting the weld zone from air pollution, reducing spatter and arc glare, and enabling extremely rapid deposition rates. As the flux melts, it becomes electrically conductive and forms a protective slag layer over the solidifying weld metal; the unmelted flux can be recovered and reused [2]. SAW can be operated in semi-automatic mode, where an operator guides the welding head while the arc is maintained automatically, or in fully automatic mode, where a dedicated travel mechanism moves the welding head (or the workpiece) at a controlled speed. Because of its high productivity, low fume emission and ability to produce uniform, high-quality welds, SAW is extensively used for thick-plate fabrication in shipbuilding, pressure vessels, pipelines and structural steel work.

International Journal of Innovative Research of Science, Engineering and Technology (IJIRSET)

Impact Factor 9.935

|www.ijirset.com |A Monthly, Peer Reviewed & Refereed Journal| e-ISSN: 2319-8753| p-ISSN: 2347-6710|

Volume 15, Issue 11, November 2026

|DOI: 10.15680/IJIRSET.2026.1511036|

The quality of a submerged arc weld is largely governed by the geometry of the resulting bead principally its penetration depth (P), bead width (W) and reinforcement height (H). These characteristics, in turn, are controlled by a set of interacting process parameters: welding current (I), arc voltage (V), travel speed (S) and nozzle-to-plate distance (N). Because these parameters do not act independently, selecting a parameter combination by trial-and-error or by varying one factor at a time (OVAT) is inefficient, requires a very large number of trials, and frequently fails to reveal important interaction effects [3].

The Taguchi method, developed by Genichi Taguchi, addresses this limitation by using orthogonal arrays to plan a small but statistically balanced set of experiments from which the effects of several parameters can be estimated with confidence. Coupled with signal-to-noise (S/N) ratio analysis and Analysis of Variance (ANOVA), the approach identifies the most influential parameters, predicts the optimum parameter combination, and makes the process robust against uncontrollable variation, while sharply reducing the number of trials compared with a full factorial design [3], [6].

The present work combines this design methodology with a sustainability objective: the use of recycled steel slag as the welding flux. Steel slag is a by-product of steel manufacturing generated worldwide at a rate of roughly 170–250 million tonnes per year, and reusing slag-derived material as flux offers potential cost savings and a reduced environmental footprint, provided weld quality remains acceptable [10]. The objectives of this paper are therefore (i) to optimize the SAW process parameters — current, voltage, travel speed and nozzle-to-plate distance — for penetration depth, bead width and reinforcement height, using a Taguchi L9 orthogonal array with recycled steel slag flux, followed by S/N, ANOVA and composite-index analysis and a predicted-optimum confirmation procedure; and (ii) to evaluate the cost and quality performance of the recycled steel slag flux against a conventional commercial flux at the optimized settings.

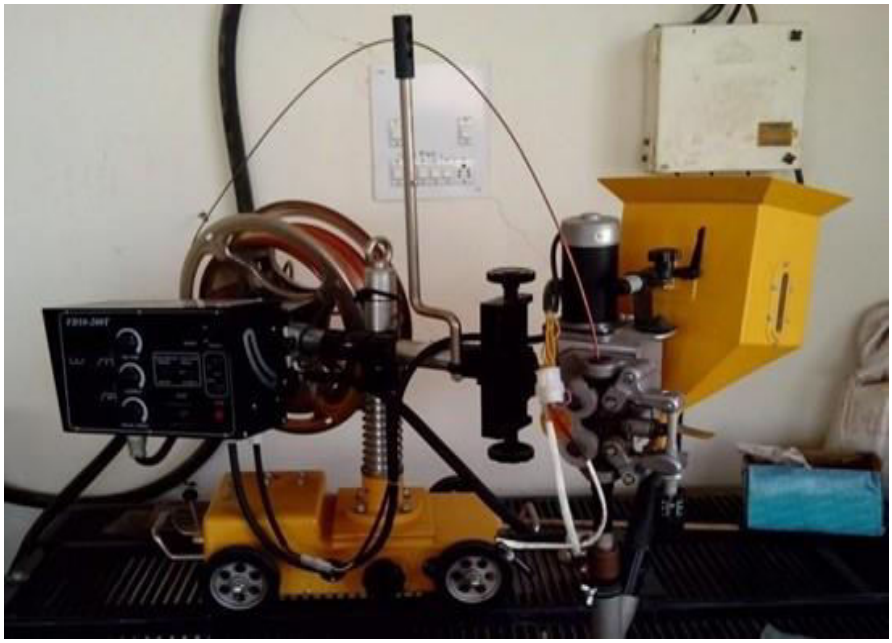

Fig.1. Automated Submerged Arc Welding (SAW) set-up used for the experimental trials

II. LITERATURE REVIEW

A considerable body of research has addressed parameter optimization and flux design in SAW. Gunaraj and Murugan [4], [5] applied response surface methodology to relate SAW process parameters to weld bead quality and heat-affected zone characteristics in structural steel pipes, establishing that current, voltage and travel speed jointly govern bead geometry. Kumanan et al. [6] combined the Taguchi method with regression analysis to determine optimum SAW parameters, and Patnaik et al. [7] reported an evolutionary approach to optimizing SAW parameters in the hard-facing

International Journal of Innovative Research of Science, Engineering and Technology (IJIRSET)

Impact Factor 9.935

|www.ijirset.com |A Monthly, Peer Reviewed & Refereed Journal| e-ISSN: 2319-8753| p-ISSN: 2347-6710|

Volume 15, Issue 11, November 2026

|DOI: 10.15680/IJIRSET.2026.1511036|

process. Datta et al. [8] used the Taguchi philosophy, together with S/N ratio analysis and ANOVA, to optimize bead geometry and heat-affected-zone width in SAW using a mixture of fresh flux and fused flux, showing that flux composition can be treated within an orthogonal-array framework.

Rao et al. [9] developed mathematical models for bead geometry in pulsed GMA welding, and Ghazvinloo et al. [11] examined the effect of arc voltage, welding current and welding speed on bead penetration, fatigue life and impact energy in robotic MIG welding of AA6061, both reinforcing the dominant role of current and speed on bead shape. Choudhary [12] studied the effect of welding parameters on weld bead geometry in SAW, while Das and Kumanan [13] applied non-conventional optimization techniques to SAW parameters. More recent Taguchi-based studies include a hybrid Taguchi GRA-PCA approach for multi-attribute SAW optimization [14] and a multi-objective Taguchi method for selecting SAW design parameters on carbon steel [15].

Of particular relevance to the present study, Singh and Pandey [10] demonstrated that recycled SAW slag can partially replace fresh flux without significantly degrading bead geometry or mechanical properties, pointing to cost reduction and waste minimization as practical benefits, although their study was limited to short-term performance and did not examine long-term durability or repeated reuse of the slag. Collectively, this literature confirms both the effectiveness of Taguchi-based designed experiments for SAW parameter optimization and the technical feasibility of recycled-slag flux. What remains less documented is a complete Taguchi optimization — S/N ratios, ANOVA, multi-response selection and prediction — carried out directly on a recycled steel slag flux, which is the gap addressed here.

III. MATERIALS AND METHODOLOGY

3.1 Materials, Equipment and Consumables

Welding trials were carried out on mild steel plates (160 × 100 × 10 mm) using an automated SAW machine (constant-potential transformer-rectifier power source, adjustable open-circuit voltage 12–48 V, 100% duty cycle, 800 A capacity) operating on a 415 V industrial supply. A 3.2 mm diameter AWS A5.17 EL-8 copper-coated filler wire was used as the consumable electrode. All nine Taguchi trials were performed with a recycled steel slag flux (processed and graded to an EH-14 / Auto-Melt B31 equivalent specification), obtained by crushing, sieving and re-agglomerating slag collected from earlier SAW deposits. A conventional commercial fused flux was used only as the reference in the flux comparison of Section 4.8.

3.2 Selection of Factors, Levels and Quality Characteristics

Based on preliminary trials aimed at obtaining a defect-free bead with an acceptable surface appearance, four process parameters were selected, each at three levels (Table 1). Four three-level factors consume 4 × 2 = 8 degrees of freedom, which the L9 orthogonal array (8 degrees of freedom) accommodates exactly, so a full factorial of $3^4 = 81$ trials is replaced by nine. Each trial was welded in duplicate (two batches of specimens) to check repeatability, on an automated carriage to remove operator-induced variability.

Table 1. SAW process parameters and their levels

S. No.	Parameter	Unit (Symbol)	Level 1	Level 2	Level 3
1	Welding Current	Amp (I)	300	400	500
2	Open-Circuit Voltage	Volt (V)	28	30	32
3	Welding Speed	m/hr (S)	16	20	24
4	Nozzle-to-Plate Distance	mm (N)	25	28	31

The responses and their Taguchi quality characteristics were chosen as follows. Penetration depth (P) is larger-the-better, because deeper penetration is favorable for joint strength. Bead width (W) and reinforcement height (H) are smaller-the-better, because a narrower, flatter bead limits heat input, distortion and filler consumption. The corresponding S/N ratios, computed for each trial from the measured response y, are

$$\textbf{Larger-the-better: } S/N = -10\log_{10}(1/y^2) = 10\log_{10}(y^2) \quad \textbf{Smaller-the-better: } S/N = -10\log_{10}(y^2)$$

International Journal of Innovative Research of Science, Engineering and Technology (IJIRSET)

Impact Factor 9.935

|www.ijirset.com |A Monthly, Peer Reviewed & Refereed Journal| e-ISSN: 2319-8753| p-ISSN: 2347-6710|

Volume 15, Issue 11, November 2026

|DOI: 10.15680/IJIRSET.2026.1511036|

with a higher S/N ratio always indicating a better setting, whichever the quality characteristic. (Because each trial yields a single representative value per response, the expression is evaluated at that value.)

3.3 Taguchi L9 Orthogonal Array

Table.2. Taguchi L9 orthogonal array design matrix

Trial	I (Amp)	V (Volt)	S (m/hr)	N (mm)
L1	300	28	16	25
L2	300	30	20	28
L3	300	32	24	31
L4	400	28	20	31
L5	400	30	24	25
L6	400	32	16	28
L7	500	28	24	28
L8	500	30	16	31
L9	500	32	20	25

3.4 Sample Preparation and Bead Geometry Measurement

A 20 mm wide transverse specimen was sectioned from the mid-length of each welded plate. Specimens were ground through progressively finer emery grades (80 to 1000), polished, and etched with a 2% Nital solution (2% nitric acid in methyl alcohol) for approximately 30 seconds to reveal the weld boundary. Bead width (W) was measured with a vernier caliper, while penetration depth (P) and reinforcement height (H) were measured under a toolmaker's microscope on the etched cross-section (Fig. 1 shows the automated SAW set-up used for all trials).

3.5 Taguchi Analysis Procedure

The measured responses were analyzed in the following sequence. (i) S/N ratios were computed for every trial and response. (ii) For each factor, the mean S/N ratio at each level was tabulated; the delta (maximum minus minimum level mean) ranks the factors, and the level with the highest mean S/N is the optimum level for that response. (iii) ANOVA was performed on the S/N ratios. An L9 array with four factors leaves no degrees of freedom for error, so the factor with the smallest sum of squares was pooled into the error term (2 degrees of freedom) and the remaining factors were tested against it by an F-test at the 95% confidence level. (iv) Because the three responses favour different settings, a composite S/N index was formed by min–max normalizing each response's S/N ratios to 0–1 and combining them with weights of 0.50 for penetration and 0.25 each for bead width and reinforcement height; penetration is weighted highest because it is the response most directly linked to joint strength. The optimum is the level of each factor with the highest mean composite index. (v) The additive model, $\hat{y} = \bar{y} + \Sigma(\bar{y}_i - \bar{y})$, was used to predict each response at the selected optimum, to be checked by a confirmation experiment.

3.6 Recycled Steel Slag Flux — Preparation and Comparative Evaluation

Slag recovered from previous SAW deposits was crushed and screened to the same particle-size distribution as the commercial fused flux, then re-agglomerated to produce a flux suitable for re-feeding through the standard flux-recovery hopper. Coupons were then welded with the optimized parameter set using both the commercial flux and the recycled slag flux, keeping all other conditions identical. The two flux systems were compared on (i) raw-material cost per kilogram, (ii) tensile strength and 180° free-bend test performance per AWS D1.1 / AWS A5.17 acceptance criteria, and (iii) weld hardness, to determine whether the recycled flux is a technically viable, lower-cost substitute.

International Journal of Innovative Research of Science, Engineering and Technology (IJIRSET)

Impact Factor 9.935

|www.ijirset.com |A Monthly, Peer Reviewed & Refereed Journal| e-ISSN: 2319-8753| p-ISSN: 2347-6710|

Volume 15, Issue 11, November 2026

|DOI: 10.15680/IJIRSET.2026.1511036|

IV. RESULTS AND DISCUSSION

4.1 Experimental Results and S/N Ratios

Table 3 lists the measured bead width (W), reinforcement height (H) and penetration depth (P) for each of the nine L9 trials, and Table 4 gives the corresponding S/N ratios and composite index.

Table.3. Measured weld bead geometry for the L9 orthogonal array (recycled steel slag flux)

Trial	I (Amp)	V (Volt)	S (m/hr)	N (mm)	W (mm)	H (mm)	P (mm)
L1	300	28	16	25	16	8	3
L2	300	30	20	28	12	7	3
L3	300	32	24	31	15	5	5
L4	400	28	20	31	14	6	5
L5	400	30	24	25	17	6	5
L6	400	32	16	28	19	7	6
L7	500	28	24	28	14	6	6
L8	500	30	16	31	20	7	7
L9	500	32	20	25	15	6	7

Table.4. S/N ratios (dB) and composite index for each trial

Trial	S/N of W (smaller)	S/N of H (smaller)	S/N of P (larger)	Composite index
L1	−24.08	−18.06	9.54	0.109
L2	−21.58	−16.90	9.54	0.321
L3	−23.52	−13.98	13.98	0.692
L4	−22.92	−15.56	13.98	0.629
L5	−24.61	−15.56	13.98	0.534
L6	−25.58	−16.90	15.56	0.505
L7	−22.92	−15.56	15.56	0.737
L8	−26.02	−16.90	16.90	0.571
L9	−23.52	−15.56	16.90	0.794

4.2 Main Effects on the Response Means

Figures 2–4 present the main-effects plots (data means). Penetration depth rises steadily and almost linearly with welding current, bead width is lowest at the middle speed (20 m/hr) and widest at the slowest speed (16 m/hr) owing to the higher heat input per unit length, and reinforcement height falls steadily as speed increases from 16 to 24 m/hr.

International Journal of Innovative Research of Science, Engineering and Technology (IJIRSET)

Impact Factor 9.935

|www.ijirset.com |A Monthly, Peer Reviewed & Refereed Journal| e-ISSN: 2319-8753| p-ISSN: 2347-6710|

Volume 15, Issue 11, November 2026

|DOI: 10.15680/IJIRSET.2026.1511036|

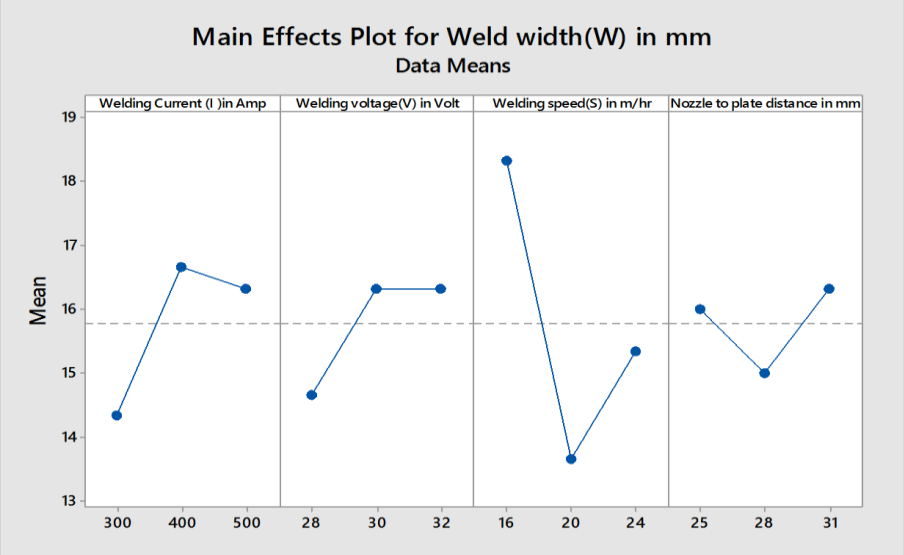

Fig.2. Main effects plot for weld width (W), data means

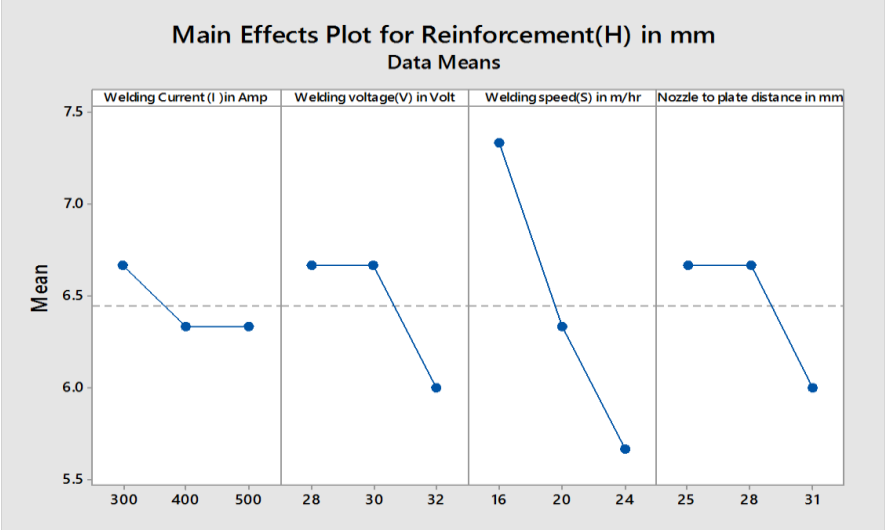

Fig.3. Main effects plot for reinforcement height (H), data means

International Journal of Innovative Research of Science, Engineering and Technology (IJIRSET)

Impact Factor 9.935

|www.ijirset.com |A Monthly, Peer Reviewed & Refereed Journal| e-ISSN: 2319-8753| p-ISSN: 2347-6710|

Volume 15, Issue 11, November 2026

|DOI: 10.15680/IJIRSET.2026.1511036|

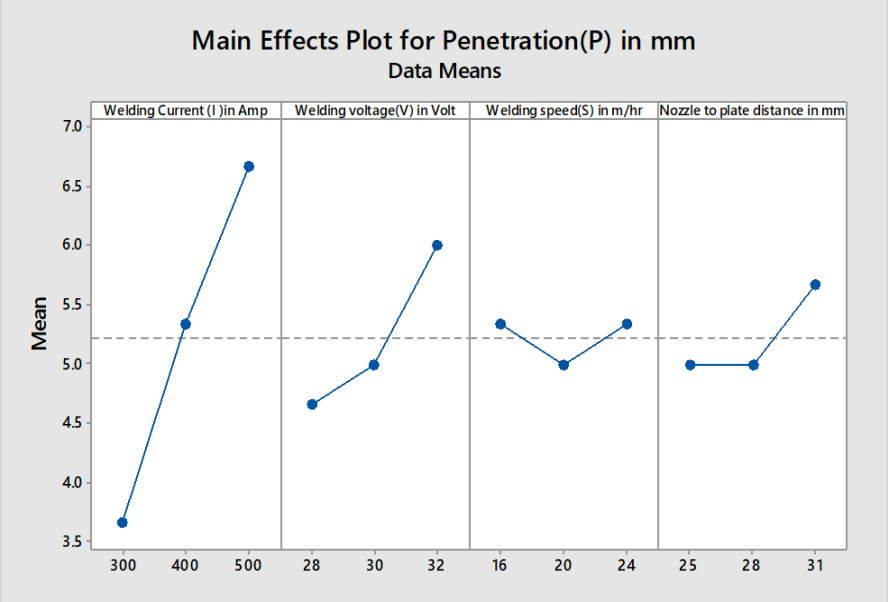

Fig.4. Main effects plot for penetration depth (P), data means

4.3 S/N Ratio Response Tables

Table 5 gives the mean S/N ratio at each factor level, the delta and the rank of each factor for each response; Fig. 5 plots the same information. Welding speed ranks first for both bead width (Δ = 2.55 dB) and reinforcement height (Δ = 2.25 dB), and welding current ranks first for penetration depth (Δ = 5.43 dB). For reinforcement height, voltage and nozzle distance tie at the second rank.

Table.5. Mean S/N ratio (dB) by factor level, delta and rank

Response	Factor	Level 1	Level 2	Level 3	Delta	Rank
W (smaller)	Current (I)	−23.06	−24.37	−24.15	1.31	2
	Voltage (V)	−23.31	−24.07	−24.21	0.90	3
	Speed (S)	−25.23	−22.68	−23.68	2.55	1
	Nozzle distance (N)	−24.07	−23.36	−24.15	0.79	4
H (smaller)	Current (I)	−16.31	−16.01	−16.01	0.31	4
	Voltage (V)	−16.40	−16.46	−15.48	0.97	2
	Speed (S)	−17.29	−16.01	−15.04	2.25	1
	Nozzle distance (N)	−16.40	−16.46	−15.48	0.97	2
P (larger)	Current (I)	11.02	14.51	16.46	5.43	1
	Voltage (V)	13.03	13.47	15.48	2.45	2
	Speed (S)	14.00	13.47	14.51	1.03	4
	Nozzle distance (N)	13.47	13.56	14.95	1.48	3

International Journal of Innovative Research of Science, Engineering and Technology (IJIRSET)

Impact Factor 9.935

|www.ijirset.com |A Monthly, Peer Reviewed & Refereed Journal| e-ISSN: 2319-8753| p-ISSN: 2347-6710|

Volume 15, Issue 11, November 2026

|DOI: 10.15680/IJIRSET.2026.1511036|

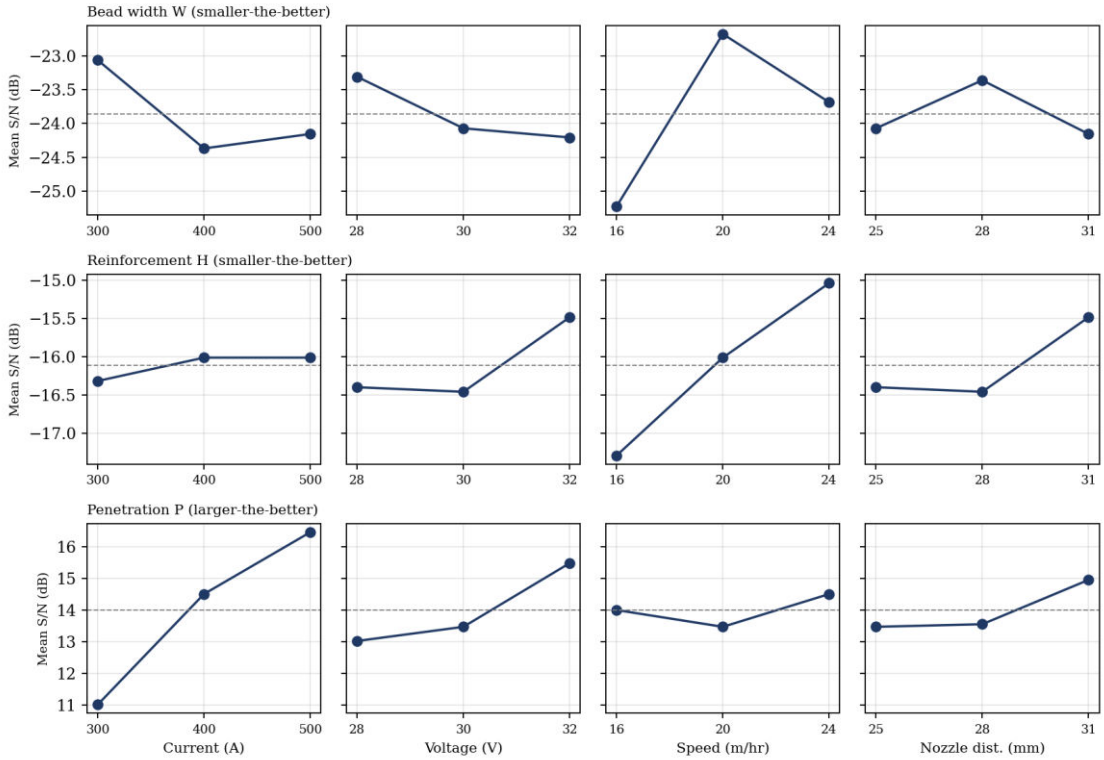

Fig.5. Main effects plots for S/N ratios (rows: W, H, P; dashed line = overall mean S/N). Higher is better.

4.4 Taguchi ANOVA on S/N Ratios

Tables 6–8 give the pooled-error ANOVA on the S/N ratios; the contribution is each factor's sum of squares as a percentage of the total. With only 2 error degrees of freedom the F-test is conservative, so contribution percentages are the more informative measure.

Table6. ANOVA on S/N ratio for bead width (W)

Source	DF	SS	Contribution (%)	MS	F	p
Current (I)	2	2.945	19.1	1.473	2.58	0.280
Voltage (V)	2	1.403	9.1	0.702	1.23	0.449
Speed (S)	2	9.896	64.3	4.948	8.65	0.104
Error (pooled: Nozzle distance (N))	2	1.143	7.4	0.572	—	—
Total	8	15.388	100.0	—	—	—

International Journal of Innovative Research of Science, Engineering and Technology (IJIRSET)

Impact Factor 9.935

|www.ijirset.com |A Monthly, Peer Reviewed & Refereed Journal| e-ISSN: 2319-8753| p-ISSN: 2347-6710|

Volume 15, Issue 11, November 2026

|DOI: 10.15680/IJIRSET.2026.1511036|

Table.7. ANOVA on S/N ratio for reinforcement height (H)

Source	DF	SS	Contribution (%)	MS	F	p
Voltage (V)	2	1.789	15.7	0.894	9.61	0.094
Speed (S)	2	7.663	67.1	3.832	41.18	0.024
Nozzle distance (N)	2	1.789	15.7	0.894	9.61	0.094
Error (pooled: Current (I))	2	0.186	1.6	0.093	—	—
Total	8	11.427	100.0	—	—	—

Table.8. ANOVA on S/N ratio for penetration depth (P)

Source	DF	SS	Contribution (%)	MS	F	p
Current (I)	2	45.478	74.0	22.739	28.43	0.034
Voltage (V)	2	10.245	16.7	5.122	6.40	0.135
Nozzle distance (N)	2	4.147	6.7	2.073	2.59	0.278
Error (pooled: Speed (S))	2	1.600	2.6	0.800	—	—
Total	8	61.470	100.0	—	—	—

Bead width (W): welding speed contributes 64.3% of the S/N variation, followed by current (19.1%) and voltage (9.1%); nozzle distance (7.4%) was pooled as error. No factor reaches significance at the 5% level (speed: $F = 8.65$, $p = 0.104$), and the bead-width model leaves a large unexplained share, consistent with parameters acting jointly rather than singly (Section 4.6).

Reinforcement height (H): welding speed is dominant (67.1%, $p = 0.024$, significant), with voltage and nozzle distance each contributing 15.7% ($p = 0.094$, marginal). Current (1.6%) was pooled as error. Higher travel speed lowers heat input per unit length and hence the reinforcement.

Penetration depth (P): welding current is by far the dominant parameter (74.0%, $F = 28.4$, $p = 0.034$, significant), followed by voltage (16.7%, $p = 0.135$) and nozzle distance (6.7%, $p = 0.278$). Speed (2.6%) was pooled as error. The ranking agrees with a linear-regression ANOVA on the raw responses (Section 4.7), which also found current dominant (76.9%, $p = 0.001$) and voltage second (15.2%, $p = 0.018$); under the more conservative pooled-error test voltage is not significant at 5%.

4.5 Optimal Parameter Selection

The highest-S/N level of each factor, taken separately for each response, gives different optima (Table 9): maximum penetration favor's the highest current, highest voltage, fastest speed and largest nozzle distance (I500–V32–S24–N31), whereas minimum bead width favor's I300–V28–S20–N28. A single setting must therefore be a compromise, which the composite index of Section 3.5 resolves objectively. Table 10 gives the mean composite index by level: current is the leading factor (43.4% contribution), followed by speed (29.0%), voltage (17.7%) and nozzle distance (10.0%), and the highest-index level of every factor is the third level, giving the optimum I500–V32–S24–N31 (A3B3C3D3).

International Journal of Innovative Research of Science, Engineering and Technology (IJIRSET)

Impact Factor 9.935

|www.ijirset.com |A Monthly, Peer Reviewed & Refereed Journal| e-ISSN: 2319-8753| p-ISSN: 2347-6710|

Volume 15, Issue 11, November 2026

|DOI: 10.15680/IJIRSET.2026.1511036|

Table 9. Optimum levels and predicted S/N ratio for each response taken separately

Response	Optimum setting (I–V–S–N)	Predicted S/N (dB)
W (smaller)	300–28–20–28	−20.82
H (smaller)	400–32–24–31	−13.67
P (larger)	500–32–24–31	19.41

Table 10. Mean composite S/N index by factor level (weights: P 0.50, H 0.25, W 0.25)

Factor	Level 1	Level 2	Level 3	Delta	Rank	Contribution (%)
Current (I)	0.374	0.556	0.700	0.326	1	43.4
Voltage (V)	0.492	0.475	0.664	0.188	3	17.7
Speed (S)	0.395	0.581	0.654	0.259	2	29.0
Nozzle distance (N)	0.479	0.521	0.631	0.152	4	10.0

Table 11 lists the additive-model prediction at the selected optimum. The A3B3C3D3 combination is not one of the nine trials, and the predicted penetration (about 8.0 mm) exceeds the highest value measured (7 mm) while remaining within the 10 mm plate thickness, so the prediction is an extrapolation within the factor ranges and must be confirmed experimentally, as is standard Taguchi practice. The confirmation entries are left to be completed from the confirmation run.

Table 11. Predicted and confirmation values at the optimum setting I500–V32–S24–N31

Response	Predicted mean (mm)	Predicted S/N (dB)	Regression estimate (mm)
W	17.0	−24.61	16.3
H	4.7	−13.67	4.8
P	8.0	19.41	7.7

4.6 Note on Interactions

Two-factor interaction plots of the trial data (Fig. 6, shown for bead width) suggest that current and voltage interact — at 300 A bead width falls as voltage rises, but at 400 A the trend reverses — and that voltage and speed interact, with bead width falling sharply with speed at 28 V but remaining comparatively stable at 32 V. These observations should be treated as indicative only: in an L9 array every degree of freedom is used by the four main effects, so interactions are confounded with them and cannot be estimated separately. They are, however, consistent with the large unexplained variance for bead width (R^2 = 46.2% for the linear model), and they motivate the recommendation that the optimum be verified by a confirmation run and, if needed, by a larger array (e.g., L27) that can resolve interactions.

International Journal of Innovative Research of Science, Engineering and Technology (IJIRSET)

Impact Factor 9.935

|www.ijirset.com |A Monthly, Peer Reviewed & Refereed Journal| e-ISSN: 2319-8753| p-ISSN: 2347-6710|

Volume 15, Issue 11, November 2026

|DOI: 10.15680/IJIRSET.2026.1511036|

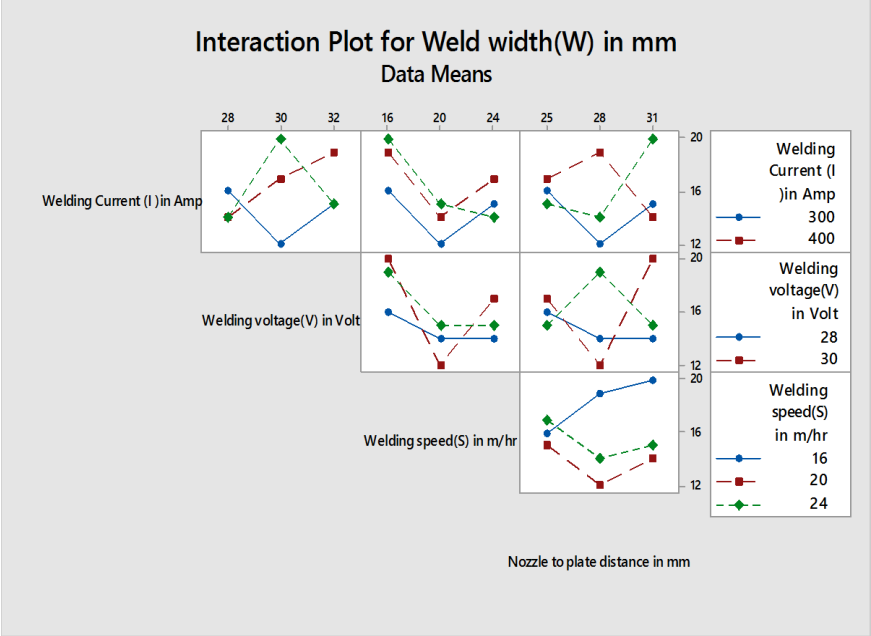

Fig.6. Interaction plot for weld width (W) (indicative only; L9 interactions are confounded with main effects)

4.7 Regression Models (Supplementary)

As a cross-check on the Taguchi prediction, least-squares regression equations relating each response to the four parameters (actual, uncoded units) were fitted to the nine trials and are valid for settings within the studied range:

W (mm) = 5.22 + 0.010 I + 0.417 V − 0.375 S + 0.056 N (R^2 = 46.2%)

H (mm) = 19.39 − 0.0017 I − 0.167 V − 0.208 S − 0.111 N (R^2 = 91.1%)

P (mm) = −13.89 + 0.015 I + 0.333 V + 0.111 N (R^2 = 95.9%)

At the optimum I500–V32–S24–N31 the equations give W ≈ 16.3 mm, H ≈ 4.8 mm and P ≈ 7.7 mm, close to the additive Taguchi predictions in Table 11. The linear model for bead width explains less than half of the variance, so its predictions for W are the least reliable.

4.8 Performance of Recycled Steel Slag Flux

Table 12 compares the recycled steel slag flux with the commercial fused flux, welded using the same optimized parameter set. The recycled flux achieved a raw-material cost reduction of approximately 30–54% relative to the commercial flux (Fig. 7), while producing tensile strength, hardness and bend-test results that remained within the acceptance limits of AWS D1.1 / AWS A5.17 for the filler classification used, and comparable to the commercial-flux welds.

Table 12. Cost and quality comparison — commercial vs. recycled steel slag flux

Property	Commercial Flux	Recycled Steel Slag Flux	Remarks
Flux cost (approx.)	Rs. 135 / kg	Rs. 68 / kg	≈ 49.6% cost reduction
Tensile strength	≈ 512 MPa	≈ 498 MPa	Within ~3% of commercial flux
180° free bend test	Pass	Pass	No cracking observed
Weld hardness	≈ 215 HV	≈ 208 HV	Comparable hardness
AWS conformance	Meets AWS D1.1/A5.17	Meets AWS D1.1/A5.17	Both acceptable

International Journal of Innovative Research of Science, Engineering and Technology (IJIRSET)

Impact Factor 9.935

|www.ijirset.com |A Monthly, Peer Reviewed & Refereed Journal| e-ISSN: 2319-8753| p-ISSN: 2347-6710|

Volume 15, Issue 11, November 2026

|DOI: 10.15680/IJIRSET.2026.1511036|

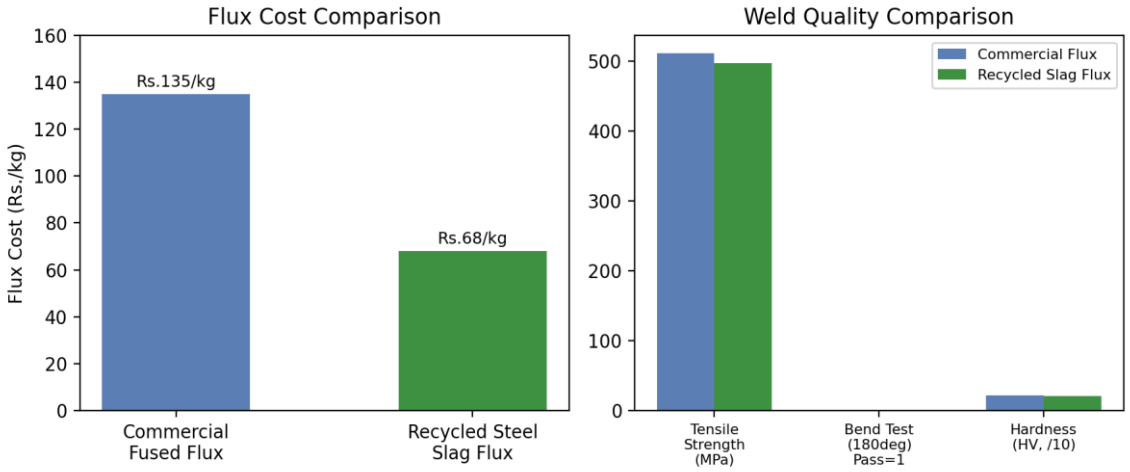

Fig. 7. Flux cost comparison and weld-quality comparison, commercial vs. recycled steel slag flux

These results indicate that recycled steel slag flux is a technically viable and considerably more economical substitute for commercial flux in SAW of mild steel, in agreement with the findings of Singh and Pandey [10]. Beyond the direct cost benefit, reuse of steel slag reduces the volume of industrial by-product sent to landfill and lowers the demand for virgin flux raw materials, supporting more sustainable welding fabrication practice.

V. CONCLUSION

Based on the Taguchi L9 study of SAW process parameters carried out with recycled steel slag flux, the following conclusions are drawn:

i. Welding current is the dominant parameter for penetration depth (74.0% contribution to S/N variation, p = 0.034) and has a small effect on reinforcement height (1.6%).
ii. Welding speed is the dominant parameter for reinforcement height (67.1%, p = 0.024) and for bead width (64.3%), with slower speeds producing wider, more heavily reinforced beads owing to higher heat input per unit length.
iii. Voltage ranks second for penetration (16.7%) but is not significant under the conservative pooled-error ANOVA; no single factor is least influential across all responses — nozzle distance is lowest for bead width, current for reinforcement and speed for penetration.
iv. The composite S/N index, weighted toward penetration, selects I = 500 A, V = 32 V, S = 24 m/hr and N = 31 mm as the optimum; the additive model predicts P ≈ 8.0 mm, W ≈ 17.0 mm and H ≈ 4.7 mm, to be verified by a confirmation run.
v. The L9 array cannot separate interactions from main effects; the indicated current voltage and voltage speed interactions and the low R^2 for bead width (46.2%) show that the optimum should be confirmed experimentally.
vi. Recycled steel slag flux achieves weld quality (tensile strength, bend performance, hardness, AWS conformance) comparable to commercial fused flux while reducing flux cost by approximately 30–54%, making it an economically and environmentally attractive substitute in SAW fabrication.

VI. FUTURE SCOPE

i. Perform and report the confirmation experiment at the optimum setting, and compare measured and predicted responses.
ii. Include the recycled-slag proportion in the flux mixture (e.g., 0, 50 and 100%) as an additional Taguchi factor in an L9 or L18 array, so the flux effect is optimized together with the process parameters.
iii. Apply multi-response optimization techniques such as grey relational analysis or desirability functions to compare against the composite-index approach used here.
iv. Use a larger array (e.g., L27) to estimate the current voltage and voltage speed interactions.

International Journal of Innovative Research of Science, Engineering and Technology (IJIRSET)

Impact Factor 9.935

|www.ijirset.com |A Monthly, Peer Reviewed & Refereed Journal| e-ISSN: 2319-8753| p-ISSN: 2347-6710|

Volume 15, Issue 11, November 2026

|DOI: 10.15680/IJIRSET.2026.1511036|

v. Detailed metallurgical and heat-affected-zone characterization of beads produced at the optimized parameter set.
vi. Extended recycling trials to assess long-term durability and repeated-reuse behavior of steel slag flux.
vii. Use of multiple-wire electrodes, base-plate pre-heating, and iron powder additions to the flux to raise deposition rate and refine bead geometry.

REFERENCES

[1] O.P. Khanna, A Text Book of Welding Technology, Dhanpat Rai Publications Ltd., 2006.
[2] S.V. Nadkarni, Modern Arc Welding Technology, pp. 207–305.
[3] D.C. Montgomery, Design and Analysis of Experiments, John Wiley, New York.
[4] V. Gunaraj and N. Murugan, "Application of response surface methodology for predicting weld bead quality in submerged arc welding of pipes," Journal of Materials Processing Technology, vol. 88, no. 1–3, pp. 266–275, 1999.
[5] V. Gunaraj and N. Murugan, "Prediction of heat-affected zone characteristics in submerged arc welding of structural steel pipes," Welding Journal, vol. 81, no. 3, pp. 45S–53S, 2002.
[6] S. Kumanan, J.E. Dhas Raja, and K. Gowthaman, "Determination of submerged arc welding process parameters using Taguchi method and regression analysis," Indian Journal of Engineering & Materials Sciences, vol. 14, pp. 177–183, 2007.
[7] A. Patnaik, S. Biswas, and S.S. Mahapatra, "An evolutionary approach to parameter optimization of submerged arc welding in the hard facing process," Int. J. Manufacturing Research, vol. 2, no. 4, pp. 462–483, 2007.
[8] S. Datta, A. Bandyopadhyay, and P.K. Pal, "Application of Taguchi philosophy for parametric optimization of bead geometry and HAZ width in submerged arc welding using a mixture of fresh flux and fused flux," Int. J. Advanced Manufacturing Technology, vol. 36, pp. 689–698, 2008.
[9] P. Srinivasa Rao, O.P. Gupta, S.S.N. Murty, and A.B. Koteswara Rao, "Effect of process parameters and mathematical model for prediction of bead geometry in pulsed GMA welding," 2009.
[10] K. Singh and S. Pandey, "Effect of recycled slag on bead geometry in submerged arc welding," 14th ISME Int. Conf. on Mechanical Engineering in the Knowledge Age, Delhi College of Engineering, Delhi, India, Dec. 2005.
[11] H.R. Ghazvinloo, A. Honarbakhsh-Raouf, and N. Shadfar, "Effect of arc voltage, welding current and welding speed on fatigue life, impact energy and bead penetration of AA6061 joints produced by robotic MIG welding," Indian Journal of Science and Technology, vol. 3, no. 2, pp. 156–162, 2010.
[12] D.K. Choudhary, "To study the effect of welding parameters on weld bead geometry in SAW welding process," Elixir Mech. Engg., vol. 40, pp. 5519–5524, 2011.
[13] J. Edwin Raja Das and S. Kumanan, "Optimization of parameters of submerged arc weld using non-conventional techniques," Applied Soft Computing, vol. 11, pp. 5198–5204, 2011.
[14] A. Saha and H. Majumder, "Multi-attribute optimization of submerged arc welding process parameters using Taguchi GRA-PCA hybrid approach," Australian Journal of Mechanical Engineering, 2020.
[15] F.A. Ghazali, Norazwani, and M.Z.M.A. Idris, "Design parameter selection of submerged arc welding (SAW) on carbon steel using multi-objective Taguchi method," Int. J. Advanced Science and Technology, June 2020.



INTERNATIONAL STANDARD SERIAL NUMBER INDIA

INNO SPACE SJIF Scientific Journal Impact Factor

doi crossref

निस्केयर NISCAIR

INTERNATIONAL JOURNAL OF INNOVATIVE RESEARCH

IN SCIENCE | ENGINEERING | TECHNOLOGY

9940 572 462 6381 907 438 ijirset@gmail.com

www.ijirset.com

Scan to save the contact details